Journal of Hazardous Materials 504 (2026) 141180

Contents lists available at ScienceDirect

Journal of Hazardous Materials

journal homepage: www.elsevier.com/locate/jhazmat

Uncovering UK coastal legacy wastes and their potential contaminant release risks through mineralogy and geochemistry

Patrizia Onnis [a,b,*], Elin Jennings [a,c], Violeta Ramos [a], Alex L. Riley [d], Catherine J. Gandy [e], Rich A. Crane [a], Ian T. Burke [f], Gavyn K. Rollinson [a], Patrick Byrne [g], Bryan M. Spears [h], Justyna P. Olszewska [h], Will M. Mayes [d], Adam P. Jarvis [e], Karen A. Hudson-Edwards [a]

[a] Camborne School of Mines and Environment and Sustainability Institute, University of Exeter, Penryn Campus, UK
[b] Department of Chemical and Geological Science, University of Cagliari, Cittadella Universitaria, Monserrato, Italy
[c] W.H. Bryan Mining & Geology Research Centre, Sustainable Minerals Institute, The University of Queensland, Brisbane, Australia
[d] School of Environmental and Life Sciences, University of Hull, Kingston upon Hull, UK
[e] School of Engineering, Newcastle University, Newcastle upon Tyne, UK
[f] School of Earth and Environment, University of Leeds, UK
[g] School of Biological and Environmental Sciences, Liverpool John Moores University, Liverpool, UK
[h] UK Centre for Ecology and Hydrology, Edinburgh, UK

HIGHLIGHTS

- Coastal legacy wastes exhibit unique PTE profiles and mineral associations.
- Mineralogy reveals key controls on PTE stability in coastal waste deposits.
- Coastal erosion and geochemical shifts may trigger PTE release from minerals.
- Coal and mining wastes pose the greatest PTE release risk along the coastline.

GRAPHICAL ABSTRACT

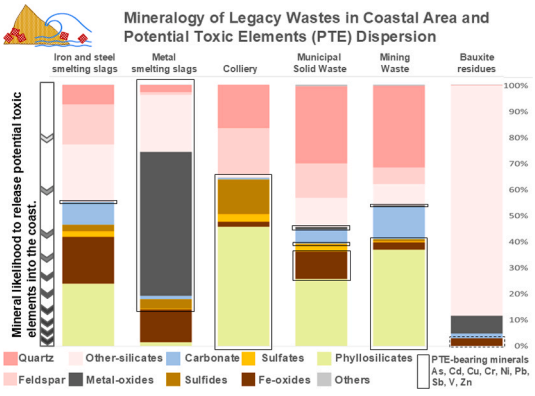

ARTICLE INFO

Keywords:
Waste management
Landfill
Contamination
Climate change
Flooding

ABSTRACT

For centuries, coastal zones have been used as disposal sites for industrial and municipal wastes, often without adequate records of their composition, raising long-term concerns regarding the potential release of contaminants. The absence of detailed mineralogical and geochemical data has limited the ability to evaluate the mobility of metal(loid)s and to design effective protection strategies. In this study, 83 samples of legacy wastes were collected from coastal sites in England, Wales, and Scotland to investigate the influence of mineralogy on the release of potentially toxic elements (PTEs). Samples were collected from 18 priority sites, selected to be

* Corresponding author at: Camborne School of Mines and Environment and Sustainability Institute, University of Exeter, Penryn Campus, UK.
E-mail address: patrizia.onnis@unica.it (P. Onnis).

https://doi.org/10.1016/j.jhazmat.2026.141180
Received 21 August 2025; Received in revised form 30 December 2025; Accepted 15 January 2026
Available online 20 January 2026

representative of the major legacy waste types found along the UK coastline. Non-ferrous slags displayed variability in mineralogy and PTE concentrations, including As, Cd, Cr, Cu, Ni, Pb, Sb, V, and Zn. These elements were predominantly hosted in stable silicates (e.g., sorosilicates, olivine) and oxides (e.g., cassiterite, spinel), with minor associations in sulfides, sulfates, and carbonates. Coal and metal mining wastes contained PTEs in redox-sensitive sulfides and secondary phases such as sulfates and iron oxides, representing the highest potential for contaminant release under seawater inundation and erosion. Bauxite waste exhibited the greatest median concentrations of Cr and V, whereas municipal solid wastes were enriched in Pb and Ni compared to ferrous slags and colliery wastes, with Ni median concentrations being the highest among all waste types. These insights emphasise the importance of mineralogical characterisation in assessing risks and managing coastal legacy wastes under climate change scenarios.

1. Introduction

Coastal zones have consistently attracted human activities, infrastructure developments, and economic endeavours, resulting in large-scale disposal of various solid wastes [1]. Particularly before the mid-1970s, in the absence of legislation and proper environmental disposal practices, dispersal of landfill contaminants relied mainly on natural dilution and dispersion through tidal flushing, as well as a range of geochemical processes including adsorption, desorption, ion exchange, and colloid transport in surrounding soils and sediments [2–4]. Coastal areas face elevated future risks of tidal flooding, saline intrusion, and erosion, all of which can enhance waste dispersion and contaminant release [5,6].

The need for a synergistic approach to quantify the contaminants held in legacy wastes and associated risks at national and global scales was highlighted in the early 21st Century [7,8]. Limitations in scientific and economical resources require a framework for site prioritisation based on multicriteria analysis. Understanding which criteria best describe and quantify contamination risks requires knowledge of sources, and dispersion processes and pathways, and potential exposure of economic, social, and ecological elements [9,10]. Riley et al. [9] showed that out of approximately 30,280 historical landfills reported in England and Wales, about 3220 were situated within 2 km of the coastline, herein named the coastal zone. Of these, approximately 700 sites lacked coastal defences or flood mitigation measures, and about 2550, though receiving some degree of protection, exhibited signs of erosion and potential contaminant transfer [9,11].

Legacy wastes contain various types of inorganic and organic hazardous materials, including polycyclic aromatic hydrocarbons (PAHs), persistent organic pollutants (POPs), plastics, asbestos, and potentially toxic elements (PTEs) [12-14]. The latter are a common problem among legacy wastes, are found in wide concentration ranges and may show variable mobility in coastal environments [5,15–18]. PTEs can be found in metallic or ionic form, with elements such as As, Cr, Sb, and V also existing in various valence states. Their mobility depends on the mineral stability, redox, pH, EC, and biological activity [15,19]. When above threshold limits, PTE concentrations can pose serious risks to human health and the environment. For example, As and Sb toxicity can lead to serious neurologic and carcinogenic effects [20,21], and Cd, Cr(VI) and Pb are known carcinogens and are toxic to plants, animals, and bacteria [22–24]. Vanadium also exhibits toxicity, though it is dose-dependent and is not classified as a human carcinogen [25]. Copper and Zn are fundamental micronutrients, although anthropogenic sources can exhibit phytotoxic effects and enter the food chain through root accumulation (e.g., [26,27]). Nickel toxicity poses various health risks to humans, including allergies, cardiovascular and renal diseases, lung fibrosis, and cancers [28]. Sea- and transitional-water environments add additional complexity to PTEs metal mobility and bioavailability limiting the understanding of PTE adverse effects on organisms [18].

In coastal environments, legacy waste dispersion pathways can be driven by physical processes such as erosion and transport in the seawater column, transitional or seawater intrusion [29,30], and desorption, complexation, cation exchange, and dissolution reactions [15,16,18]. Abundant seawater ions such as Na, K, Mg and Ca can participate in cation exchange with weakly bound PTEs (e.g. Ni, Cu, Cu, Cd, Zn and As) [31,32]. Seawater Cl can form complexes with Cd, Zn, and Pb, increasing their mobility [33]. Furthermore, prolonged seawater intrusion can generate reducing conditions due to oxygen consumption exacerbated by microorganisms [34]. Such conditions can promote microbially-mediated reduction of Fe and Mn hydroxides and sulfates and cause release of their sorbed or co-precipitated PTEs [15]. Metal-rich sulfides and other reduced minerals, when oxidised, can become unstable and release PTE [35]. Although dilution with seawater can play a fundamental role in decreasing PTE concentrations, bioaccumulation and biomagnification through bottom sediment ecosystems and food chain remain a risk for systems exposed to these elements [18].

Remediation and monitoring prioritisation frameworks based on national-scale source-pathway-receptor conceptual models are fundamental to offering a response to legacy wastes contamination hazards [1,9]. However, mineralogical and geochemical characterisations are scarce, limiting the understanding of contaminant occurrence and behaviour in legacy wastes and remediation prioritisation. Legacy wastes posing potential contamination risks to human and ecosystem receptors include municipal solid wastes (often mixtures of industrial, commercial, and household), mining wastes (metal and coal), slags (ferrous, steel, and non-ferrous), and bauxite residues (Table S1). PTE geochemistry and potential release mechanisms in such legacy wastes have been, and still are researched, but a systematic mineralogical and geochemical comparison among and within the different types is still missing.

This research aimed to provide a comprehensive mineralogical and geochemical characterisation of legacy wastes and the risk they may pose to the coastal environment. Given the extensive industrial history and variety of wastes disposed of in the coastal zone that pre-date environmental regulation, this research focuses on the UK coastline and provides a valuable baseline to consider the environmental risks of similar coastal wastes on a global basis [36]. The specific objectives were to: i) characterise the bulk mineralogy and geochemistry of the legacy wastes; ii) quantify PTEs (namely As, Cr, Cu, Cd, Ni, Pb, Sb, V, and Zn) and identify their host minerals; iii) understand the potential environmental risks posed by legacy wastes; iv) generate a comprehensive mineralogical and geochemical database that can feed into national scale remediation and monitoring programs. This comparative analysis can inform environmental regulators and practitioners and benefit the international community affected by the global challenge of coastal legacy wastes.

2. Materials and methods

2.1. Study sites, sample collection, and preservation

Along the UK coastline, legacy wastes sample sites were identified from national-scale databases [9]. Selection of priority sites for this study followed a multi-criteria decision analysis based on 1) coastal erosion susceptibility, 2) risk of tidal inundation, 3) receptor distance, and 4) distance from the coast. This approach, detailed in Riley et al. [9], was designed to identify sites that are representative of the major legacy

wastes challenges facing the UK coastline. Legacy wastes were grouped into waste types based on records of their sources, locations, and potential hazards reported in literature or highlighted by local authorities and environmental consultants. The legacy waste types selected were non-ferrous slags (Me-SS), ferrous (steel and iron) slags (Fe-SS), municipal landfill (municipal/commercial/industrial) (MSW), bauxite residues (BR), coal waste (CW), and metal mine waste (MW) (Table S1). Across the various waste types, 18 priority sites were selected, and a total of 83 solid samples were collected (Fig. 1). To maximise the representativeness of the sampling, each sample was collected as a composite of five increments from around a 10 m^2 area [37]. Sediment particles > 2 cm in diameter and vegetation residues were removed, and about 500 g of material was collected in pre-cleaned, single-use polyethylene bags to minimize the risk of contamination. The samples were air-dried at 30 °C and rifled into aliquots. For geochemical and powder diffraction analysis, an aliquot of 50 g was mechanically ground to less than 125 μm with a tungsten carbide mill. Although such a mill could introduce trace W or Co, these elements were not analytes of interest in this study.

2.2. Mineralogical analysis

The mineralogical compositions of the samples were determined by X-ray diffraction (XRD) using a Siemens D500 diffractometer with an X-Ray tube at 1.5 kW and Cu-anode. Diffractograms were acquired for the ground samples (<125 μm) in the 2–70° 2θ range, at 1-second per step and with a step size 0.02°2θ. The resultant spectra were interpreted with Bruker software EVA v.18.0.0.0. and the JCPDS PDF-2 (2004) database. The spectra position was verified against a quartz standard (ICDD PDF-2 card 46–1045).

Mineral morphology, association and quantification were determined for 30 samples with representative PTE concentrations. For these samples, 30 mm diameter epoxy resin blocks were prepared using approximately 1 g of material of < 2 mm diameter. The blocks were coated with a 25 nm layer of carbon and analysed with a QEMSCAN® 4300 automated scanning electron microscope. This instrument was operated at 25 kV and 5 nA beam using a tungsten filament under high vacuum and an X-ray count rate of 1000 counts (10 ms on average) from four EDS Bruker SDD detectors [38]. The Fieldscan measurement mode was applied with a 10 μm X-ray pixel spacing resolution. The QEMSCAN output included false colour images that enhanced a visual inspection of the phase distributions. The percentage of the polished area covered by particular minerals was considered to be the abundance of that mineral in the given sample. Limitations due to the analysis being confined to a 2D block surface, and the resolution step which resulted in mixed spectra for phases smaller than 10 μm, were considered in the data analysis. Phases observed via QEMSCAN were assigned to minerals based on their chemical composition and XRD data. Limits of the detections were 1 vol%.

Scanning Electron Microscope (SEM) investigations focused on PTE-bearing minerals. A TESCAN Vega 3 SEM (high vacuum mode, accelerating voltage of 20.0 kV incorporating an X-Ray Energy Dispersive Spectrometer (EDS) with an Oxford EDS system (XMax 80 mm EDS) and Aztec software (version 3.3 SP1) was used for chemical spot analysis and chemical mapping. Samples were coated to 25 nm with a carbon thin film using an Agar Automatic carbon coater.

2.3. Geochemical analysis

Elemental compositions of the ground samples were acquired through a portable Olympus Delta X-Ray Fluorescence (pXRF) analyser and total acid digestion and ICP analysis. The elements analysed were Al, Ca, Fe, K, Mg, and Na (major elements), and As, Cd, Cr, Cu, Ni, Pb, Sb, V, and Zn (potentially toxic elements, PTE). These PTEs were selected due to their known ecotoxicities, and probable occurrence in the investigated waste types [39,40,14,41]. PTEs such as Hg, U, and Th which may be present in specific wastes were not analysed in this study. pXRF analysis allowed for an initial screening of elemental composition and selection of representative samples for total acid digestion and detailed mineralogical investigations. The pXRF was calibrated at the beginning, middle and end of every session with a silver standard (315 Olympus), and data quality was evaluated by running samples in triplicate to determine precision, and silica blank and certified reference materials (CRMs) for accuracy. The CRMs used were RTS-3a (sulfide ore mill tailings certified by the Mining and Mineral Sciences Laboratories, CANMET, Canada), SRM 2710 (Montana I Soil certified by National Institute of Standards and Technology, USA) and 73305 China National Analysis Centre for Iron and Steel approved material. To account for

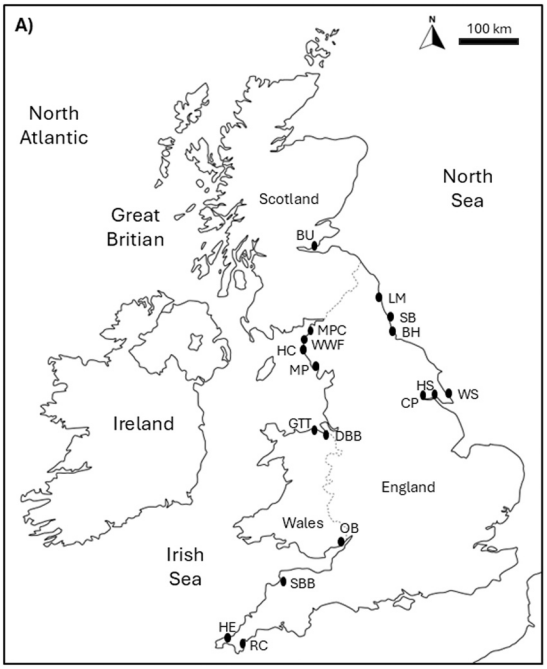

Waste type	Site	N'Samples	Location
Colliery waste (CW)			
	(BH)Blackhall	4	54°45'07"N, 001°16'56"W
	(HC)Haig Colliery	4	54°32'25"N , 003°36'01"W
	(GTT)Gas Terminal Talacre	2	53°20'44"N , 003°18'45"W
	(SB)Seaham Blast beach	2	54°49'22"N , 001°19'15"W
	(LM)Lynemouth	4	55°13'09"N , 001°31'42"W
Municipal Solid Wastes (MSW)			
	(DBB)Dee Bank Bagillt	2	53°16'33"N , 003°10'24"W
	(HS)Hessle Tip	4	53°43'01"N , 000°25'52"W
	(WS)Withernsea Landfill	5	53°44'30"N , 000°01'17"E
	(OB)Oldbury-on-Severn	2	51°39'09"N , 002°34'17"W
	(SBB)Seven Brethren Bank	3	51°04'29"N , 004°03'21"W
Mining Wates (MW)			
	(HE)Hayle Estuary	3	50°10'59"N , 005°26'05"W
	(RC) Restronguet	3	50°12'41"N, 005°05'56"W
Non-ferrous (metal) smelting slags (Me-SS)			
	(CP)Capper Pass	24	53°43'04"N, 000°31'37"W
	(HE)Hayle Estuary	3	50°10'59"N , 005°26'05"W
Ferrous Slags (Fe-SS)			
	(MP)Millom Pier	6	54°12'33"N, 003°15'04"W
	(MPC)Maryport Coastal	4	54°42'32"N , 003°30'37"W
	(WWF)Workington Windfarm	5	54°39'46"N , 003°33'34"W
Bauxite residues (BR)			
	(BU)Burntisland	3	56°03'34"N , 003°14'49"W

Fig. 1. Site locations and sample list.

matrix effects, accuracy was validated using the abovementioned CRMs with have different matrices. The analysis program on the pXRF was used to match the sample as close as possible (e.g. soil program for soils).

The total elemental composition was measured by Inductively Coupled Plasma Mass Spectrometry (ICP-MS, Agilent 7700) following acid digestion. 100 mg of each sample was digested progressively with: i) 4 mL HF (50 % trace metal grade), 3 mL HCl (trace metal grade) and 1 mL HNO_3 at 160 ℃ for 8 h; ii) 1 mL $HClO_4$ at 180 ℃ till dry; iii) 1 mL of HNO_3 and 5 mL deionised water at 100 ℃ for 30 min. Finally, 44 mL of deionised water was added and a 1:10 dilution (5 % HNO_3) was applied to analyse the samples on the ICP-MS. Blanks and CRMs were run with the batch of samples, and 10 % of the samples were processed in duplicate to check analysis precision. Across the waste type and sites, 25 representative samples were selected for carbon and sulfur analysis with the LECO SC-144DR analyser at Wheal Jane Services Ltd. Samples were pulverised (<45 μm) for total S, SO_4^- and S^-, total, inorganic and organic C. Data elaboration was performed with Excel 2016 and Origin Lab 2022.

The elemental concentrations did not conform to a normal distribution, so significant differences in elemental concentrations (by site and between waste types) were tested via non-parametric Kruskal-Wallis ANOVA and the post-hoc Dunn's paired comparison test (with Bonferroni correction) using Origin Lab 2022, with a significance threshold of $p < 0.05$. Values were compared to environmental quality guidelines reported by the Canadian soil guidelines for the protection of the environment and human health [42] adopted by the Environment Agency [43] due to the lack of national British standards. The CCME guidelines were selected as they provide a comprehensive and internationally recognised framework for sediment quality assessment, and they have been previously adopted for similar assessments in the UK [43].

Contaminant concentrations equal or greater than a predicted effect level (PEL) may cause adverse conditions to the ecosystem health. PEL values were not available for Sb and V and so the threshold limit concentrations for agricultural land (Agric) were used for these elements [42]. Major elements and PTE concentrations were further compared to i) literature data; ii) upper continental crust concentrations [44]; iii) UK topsoil background concentrations reported by the British Geological Survey in the work by Ander et al. [45].

3. Results

3.1. Mineralogy

Colliery wastes (CW) were dominated by silicate minerals such as quartz, feldspars (albite, orthoclase, and other K-feldspars), and phyllosilicate minerals (illite and/or muscovite, kaolinite, and chlorite) (Table 1; Fig. 2). Generally, sulfide (pyrite, sphalerite, and chalcopyrite) abundances ranged between 1 and 8 vol%, and sulfate minerals (gypsum, barite and jarosite) ranged between < 1 and 7 vol% (Table 2). Samples from Lynemouth had lower silicate contents and high amounts of pyrite (41 vol%) and clay-pyrite mixed phases (8–20 vol%). The high pyrite content was quantified by QEMSCAN® and its morphology was confirmed by SEM-EDS analysis. Iron oxides (5 vol%, magnetite and hematite) were found in samples containing mullite, a high-temperature nesosilicate. Iron oxides, sulfides, and sulfates contained PTE such as As, Zn, Cu, and Pb (Table 2). Carbonates such as calcite and ankerite were present in low amounts (<1 vol%).

Mining waste (MW) was generally composed of quartz, feldspars (orthoclase and albite), and clay minerals (illite and/or muscovite, kaolinite, and chlorite) (Table 1; Fig. 2). Silicate phases ranged around 90–95 vol% for the Restronguet Creek and 46–90 vol% for the Hayle Estuary samples. Other minerals were sulfides (pyrite, sphalerite, and chalcopyrite), sulfates (jarosite and gypsum), and halite. Arsenic-bearing arsenopyrite, scorodite, and bukovskyite were present in both locations (<1 vol%) (Table 2).

Municipal solid waste (MSW) samples had bulk mineralogical compositions similar to those of CW, and were dominated by silicate minerals (quartz, feldspar, clay, and mica minerals) (Table 1; Fig. 2). Samples from Hessle Tip were rich in Ca-feldspar (anorthite). Carbonates were ubiquitous and represented by calcite, dolomite, and ankerite. Iron oxides, such as hematite and goethite, were present especially in samples from Withernsea Landfill and accounted for up to 23 vol% of the samples. These samples also had 1 vol% of Fe-oxides mixed with metal (Cu and Zn) and sulfate phases (Table 2). Aluminium- and Ti-oxides were present in all the samples (<2 vol%).

Bauxite residues (BR) were composed of silicates (88 vol%), calcite (2 vol%), and various metal oxides (Table 1; Fig. 2). The latter included Fe oxides (hematite and goethite, 3 vol%); Ti oxides (rutile and perovskite, <1 vol%), and Al oxides (boehmite, calcium-aluminium oxides,

Table 1
Mineral distribution among waste types based on QEMSCAN analysis. Me-oxides* include metal droplets and metal oxides. See Table 2 for a complete mineral list. sdv, standard deviation; min: minimum; max: maximum. Limit of detection is 1 vol%.

	mean	sdv	min	max	mean	sdv	min	max		Mean	sdv	min	max
Mineral group (vol%)	**Fe-SS (n = 4)**				**Me-SS (n = 4)**					**CW (n = 10)**			
Quartz	**7**	3	3	11	**3**	5	< 1	11		**17**	17	2	54
Feldspar	**15**	14	1	38	**1**	1	< 1	3		**18**	15	2	55
Other silicates		**22**	22	< 1	54	**22**	32	< 1	77	**1**	1	< 1	4
Phyllosilicates	**24**	20	3	45	**2**	3	< 1	6		**46**	21	4	72
Carbonate	**9**	8	< 1	18	**1**	2	< 1	5		**< 1**	2	< 1	5
Fe-oxides	**18**	18	1	46	**13**	21	< 1	50		**2**	2	< 1	5
Me-oxides*	**< 1**	< 1	< 1	< 1	**55**	40	14	99		**< 1**	< 1	< 1	< 1
Sulfates	**2**	1	1	4	**< 1**	< 1	< 1	1		**3**	3	< 1	7
Sulfides	**3**	4	< 1	10	**4**	4	< 1	9		**13**	16	1	49
Others	**< 1**	< 1	< 1	< 1	**< 1**	< 1	< 1	< 1		**< 1**	< 1	< 1	< 1
TOT	*100*				*100*					*100*			
	MSW (n = 5)				**MW (n = 6)**					**BR (n = 1)**			
Quartz	**30**	10	15	45	**31**	12	17	47		**< 1**	n.a.	n.a	n.a.
Feldspar	**13**	2	10	15	**6**	3	2	11		**< 1**	n.a.	n.a	n.a.
Other silicates	**11**	2	9	14	**8**	4	3	14		**88**	n.a.	n.a	n.a.
Phyllosilicates	**26**	8	18	40	**37**	25	5	67		**< 1**	n.a.	n.a	n.a.
Carbonate	**5**	2	2	8	**13**	19	< 1	53		**< 1**	n.a.	n.a	n.a.
Fe-oxides	**10**	8	1	23	**3**	3	< 1	9		**3**	n.a.	n.a	n.a.
Me-oxides	**1.0**	1	< 1	2	**< 1**	< 1	< 1	1		**7**	n.a.	n.a	n.a.
Sulfates	**3**	3	< 1	7	**< 1**	< 1	< 1	1		**< 1**			
Sulfides	**< 1**	< 1	< 1	1	**< 1**	1	< 1	2		**< 1**			
Others	**< 1**	< 1	< 1	1	**0.5**	< 1	< 1	1		**< 1**	n.a.	n.a	n.a.
TOT	*100*				*100*					*100*			

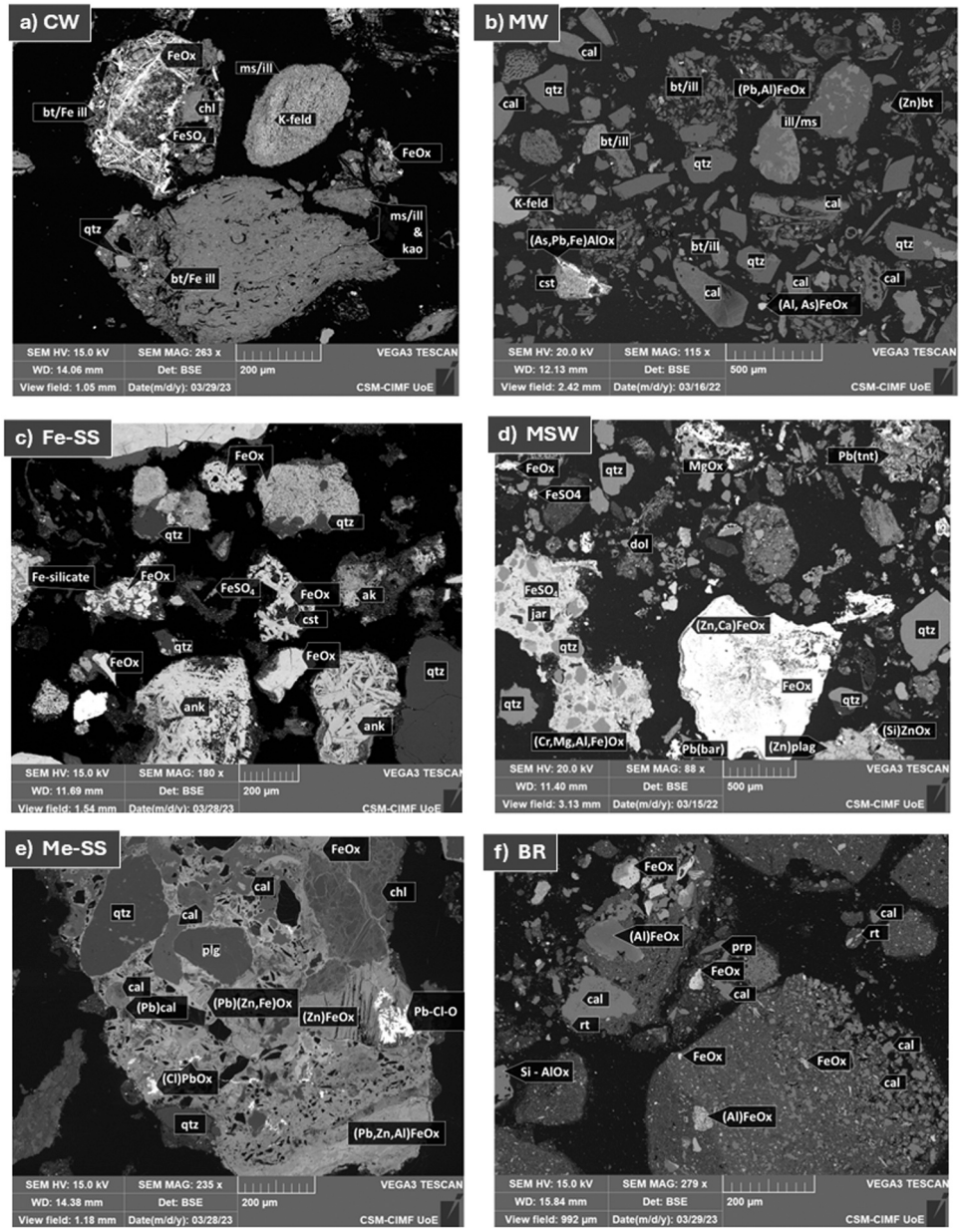

Fig. 2. SEM images of (a) CW, coal wastes, site Blackhall; (b) MW, mining waste, site Hayle; (c) iron smelting slags, Fe-SS, site Millom Pier; (d) municipal solid wastes, MSW, site Withernsea; (e) non-ferrous smelting slags, Me-SS, site Hayle; (f) bauxite residues, BR, site Burntisland. a) CW were dominated by silicates (qtz, K-feld) and secondary minerals such as phyllosilicates (ms/ill, kao, bt, chl) and iron sulfates and oxides ($FeSO_4$, FeOx) showing weathering edges. b) MW had high amounts of quartz (qtz), calcite (cal), phyllosilicates (bt/ill, ms/ill), and oxides (AlOx and FeOx). Pb, Zn, and As occurred in various phases. c) Fe-SS had Fe bearing minerals (FeOx, ank, Fe-silicate) and quartz. d) MSW had various silicate (qtz and plag) and PTE-bearing oxides and sulfate (FeOx, tnt, ZnOx, bar); e) Me-SS had silicates (qtz and plg) and PTE-bearing oxides (FeOx and PbOx) cemented together and not showing signs of alteration. f) BR was mainly comprised of calcite (cal) and oxide minerals (FeOx, AlOx, rt). Key: ak: åkermanite, ank: ankerite, bar: barite, bt: biotite, cal: calcite, chl: chlorite, cst: cassiterite, dol: dolomite, Fe-ox: iron oxides and hydroxides, ill: illite, ilm: ilmenite, jrs: jarosite, kao: kaolinite, K-feld: K-feldspar, ms: muscovite, ox: oxide, plag: plagioclase, py: pyrite, prp: pyrope, qtz: quartz, rt: rutile, zr: zircon.

6 vol%), as well as other oxide phases enriched in Fe and Ti (Table 2).

Iron and steel smelting slags (Fe-SS) were composed of silicate minerals such as quartz, feldspars (orthoclase and albite), and high-temperature silicates rich in Fe and Ca (gehlenite, ferro-åkermanite, monticellite, and hedenbergite) (Table 2; Fig. 2). Other silicates included phyllosilicate minerals (illite, muscovite, kaolinite) and biotite. The mineral distribution showed high variability among samples (Table 1). Carbonate minerals, especially calcite, were ubiquitous among the sites. Different oxides were present, namely Fe-oxides (hematite, magnetite, and franklinite), Ti-oxide (rutile), and Ca-oxide (lime) (Table 2). Other accessory minerals were sulfides (chalcopyrite and manganese sulfide), sulfate (jarosite), and salts (halite and fluorite). Occasionally, samples showed high sulfate and sulfide minerals reaching 10 vol%.

Non-ferrous smelting slags (Me-SS) showed high mineral variability within and among sites (Table 1; Fig. 2). Generally, they had similar silicate minerals but lower Ca concentrations compared to ferrous slag. High temperature silicate minerals were the olivine-group minerals (fayalite, forsterite), mullite, and sodalite (Table 2). A range of different metal oxides and hydroxides was present. This included Fe (hematite, goethite, magnetite, and wustite), Fe and Mg (magnesioferrite), Fe and Mn (jacobsite), Mg (brucite), Mg and Al (spinel), Cu (paramelaconite),

Table 2
Mineral distribution in the various waste types. The number refers to the number of samples having the mineral characterised with XRD. Key legend: (*) minerals observed through QEMSCAN and SEM-EDS; (?) mineral only observed with SEM and EDS; (1) metal(loid) droplets or mixed with S or O; (2) As was found associated with Fe – S – O phases, and Fe - S mixed with clay minerals; (3) metal(loid) droplets or mixed with S or O; (4) SEM analysis highlighted the presence of Cu, Cr, and Ni in O - Mg - Si - Fe phases; (5) SEM analysis highlighted the presence of Sn, S, and O bearing Cu, Cr, Pb. QEMSCAN reports Ni with Sn O; (6) SEM images show O:Fe:Zn phases with atomic weight ratio 5:2:1, respectively. Pink, silicates and phyllosilicates; blue, carbonates; light grey, iron oxides; grey, Me-oxides; yellow, sulfides; pale yellow, sulfates; white, other minerals.

Mineral		General Formula	CW	MW	MSW	Fe-SS	Me-SS	BR
Silicate								
	Quartz	SiO_2	15	6	14	15	6	3
Feldspar	Orthoclase	$K_2AlSi3O_8$	14	3	10	13	5	
	Albite	$Na_2AlSi_3O_8$	15	3	9	8	4	
	Anorthite	$CaAl_2Si_2O_8$	*		3			
	Microcline	$K(AlSi_3O_8)$	1					
	Sanidine	$K_2AlSi_3O_8$	1					
Olivine	Fayalite	Fe_2SiO4					1 (4) Cu, Ni, Cr, Pb	
	Forsterite	Mg_2SiO_4					1 (4) Cu, Ni, Cr, Pb	
	Monticellite	$CaMgSiO_4$				3		
Pyroxene	Hedenbergite	$CaFe(Si_2O6)$				1		
	Diopside	$CaMg(Si_2O_6)$		*	*			
Garnet	Pyrope	$Mg_3Al_2Si_3O_{12}$						1
Sorosilicate	Ferro Åkermanite	$Ca_2Fe_2{+}Si_2O_7$				4	3 Zn	
	Gehlenite	$Ca_2Al(SiAl)O_7$				5		
	Epidoto	$Ca_2Al_3Fe(SiO_4)(Si_2O_7)O(OH).$						*
Nesolicate	Mullite	$Al_6Si_2O_{13}$	3				1	
Cyclosilicate	Schorl (Tourmaline)	$NaFe^{2+}{}_3Al_6(BO_3)_3Si_6O_{18}(OH)_4$		2	*			
Tectosilicate	Sodalite	$Na_8(Al_6Si_6O_{24})Br_2$					1	
Phyllosilicate								
	Kaolinite	$Al_2(Si_2O_5)(OH)_4$	14 (2) As	5	10	3	2	
	Illite/muscovite	$KAl_2(AlSi_3O_{10})(OH)_2$	14	6	8	3	2	*
	Chlorite	$(Mg,Fe^{2+})_5Al(AlSi_3O_{10})(OH)_8$	1 (2) As	3 Cu, Zn	*			*
	Biotite	$K(Mg,Fe)_3AlSi_3O_{10}(OH)_2$		3	1	3	1	
Carbonate								
	Ankerite	$Ca(Fe^{2+},Mg)(CO_3)_2$	3		1	1	1	
	Calcite	$CaCO_3$	4	3	10	10	1 Pb	3
	Cerussite	$PbCO_3$					1	

(*continued on next page*)

Table 2 (*continued*)

			CW	MW	MSW	Fe-SS	Me-SS	BR
Fe-oxides								
	Hematite	Fe_2O_3	2 (1) Cu, Zn, Pb		5	7	5	3
	Goethite	FeO(OH)	* (1) Cu, Zn, Pb		1 Zn	*	3	3
	Magnetite	Fe_3O_4	2 (1) Cu, Zn, Pb			5	2	
	Magnesioferrite	$MgFe^{3+}{}_2O_4$					2	
	Wuestite	FeO					2	
	Iron Oxyhydroxides	e.g. Fe_2O_3*0.5H_2O; FeO(OH)·nH_2O	* (2) As (1) Cu, Zn, Pb	* Cu, As	* Zn	*		
Me-oxides*								
Spinel	Spinel	$MgAl_2O_4$					3 Cr, V, Zn	
	Jacobsite	$(Mn_{0.84}Fe_{0.16})(Mn_{0.16}Fe_{1.34}Cr_{0.5})O_4$					1 Cr	
	Franklinite	$ZnFe_2O_4$				1	? (6) Zn, Pb	
Rutile	Rutile	TiO_2			*	1		3
	Ilmenite	$FeTiO_3$		*	*	*	*	
	Cassiterite	SnO_3		* Cu, V			3 (5) Ni, Cr, Pb, Cu	
	Perovskite	$CaTiO_3$						3
	Metal(loid) oxides	(Fe,As)Ox, (Cr,Fe)Ox, PbOx		* Cr	* Cr, As, Pb			
Other Me-oxides	Paramelaconite	Cu_4O_3					1 Cu, Sb, Pb, As	
	Brucite	$Mg(OH)_2$					1	
	Boehmite	AlO(OH)						3
	Lime	CaO				1		
	Ca- and Al-Oxide	nCaO*nAl_2O_3						3
Metal(loid) droplets	Metal(loid) droplets	Cu Sn, Pb Cu, Sn, As Fe Ni			* Zn, Cu, Pb	* Cu	* (3) Cu Pb Ni Zn	
Sulfide								
	Pyrite	FeS_2	4 (2) As	1 As	* As, Zn, Pb	*	1 As	
	Galena	PbS			* Pb		* Pb	
	Sphalerite	ZnS	* Zn	* Zn	* Zn		1 Zn	
	Chalcopyrite	$CuFeS_2$	* Cu	* Cu		1	* Cu Pb	
	Troilite-2H	FeS					1	
	Mn sulfide	MnS				1		
Sulfate								
	Gypsum	$CaSO_4$·$2H_2O$	6	*	2	*	*	
	Jarosite	$KFe^{3+}{}_3[SO_4]_2(OH)_6$	1 2 (2) As	* As, Cu	*	1	1	
	Baryte	$BaSO_4$			*	*		
Others								
	Plumbogummite	$PbAl_3(PO_4)(PO_3OH)(OH)_6$		* Pb				
	Apatite	$CaPO_4$		*	*	*	*	
	Fluorite	CaF_2		*		2	1	
	Halite	NaCl		2	1	1	1	
	Scorodite	$FeAsO_4$·$2H_2O$		2 As				
	Glass			*			2	*

and Sn oxides (cassiterite) (Table 2). Carbonate minerals were mostly calcite and cerussite. Sulfide minerals comprised 4 vol% of the samples and included pyrite, trolite, and sphalerite, whereas sulfate minerals (<1 vol%) were represented by jarosite. Other accessory minerals were halite and fluorite. Non-crystalline phases such as glass and metal droplets (Pb, Zn-Cu) were observed. Capper Pass samples comprised mainly chromium spinel (69 vol%), with silicates and Fe phases accounting for less than 10 and 1 vol%, respectively. Tin phases (14 vol%), Cu phases (9 vol%), and Pb-bearing phases (1 vol%) were also present. In some samples, cassiterite accounted for 94 vol% of the sample, and were accompanied by Pb, Cu, and Fe mixed Sn-oxide phases (Table 2). Very high percentages (e.g., cassiterite accounting for 94 vol% in one sample) represented single-sample anomalies and illustrate the extreme heterogeneity within certain Me-SS waste deposits. Arsenic-bearing phases (1 vol%) were arsenopyrite, Fe-, and Sn-oxide phases, and accessory silicate minerals (<1 vol%) were present. Copper, Pb, and Ni were present in Fe-oxides and sulfate phases (Table 2).

3.2. Geochemistry

The different waste types had characteristic major elements and PTE compositions (Table S2). A comparative summary of median PTE concentrations from this study and their context within the ranges reported in the wider literature is provided in Supplementary Table S3. CW samples had the lowest Ca concentrations and an Al/Fe ratio of around 1 (Table S2.a). Total S concentrations were high, with most sulfur present as sulfide (Figure S.2). CW from Lynemouth had the highest S values among CW sites. Carbon was also elevated, with generally organic C exceeding inorganic C. MW samples were depleted in Mg, Na, and K compared to the upper crust (Figure S1). Total sulfur content was high, primarily as sulfide (Figure S2). MSW showed strong site-specific heterogeneity with significant variability for Ca, Fe, Mg, and Na (Table S2.e). Withernsea samples had high Fe, while Hessle Tip showed high Ca and Al. MSW had the second-highest total C (up to 26 wt%), mostly in organic form. Sulfur concentrations were moderate (Figure S2).

Fe-SS exhibited high variability in major elements, particularly Ca and Al (Table S2.c). Two samples were similar to CW, with low Ca and high Al. Sulfur concentrations were moderate (Figure S2). Fe-SS had compositions dominated by Fe and values close to or below upper crust concentrations. Total S was among the highest, with Capper Pass having extreme S values. Me-SS also had high organic and inorganic C. BR was characterised by high Fe, Ca, and Na, and the lowest K and Mg (Table S2f). Carbon was mostly inorganic and low in concentration (Figure S2).

Overall, all PTE types and concentrations varied among and occasionally within the waste types (Fig. 3; Table S2). Arsenic concentrations in all the wastes were enriched compared to upper continental crust (Figure S1). The highest As concentrations and variabilities occurred in the MW (median 1370 mg kg^{-1}) and Me-SS samples (median 160 mg kg^{-1}). CW, MSW, and Fe-SS samples had similar As medians (40 – 50 mg kg^{-1}) and showed less As variability compared to the other waste types.

Cadmium concentration medians were all below 1.5 mg kg^{-1}, with only the MSW samples being enriched compared to upper continental

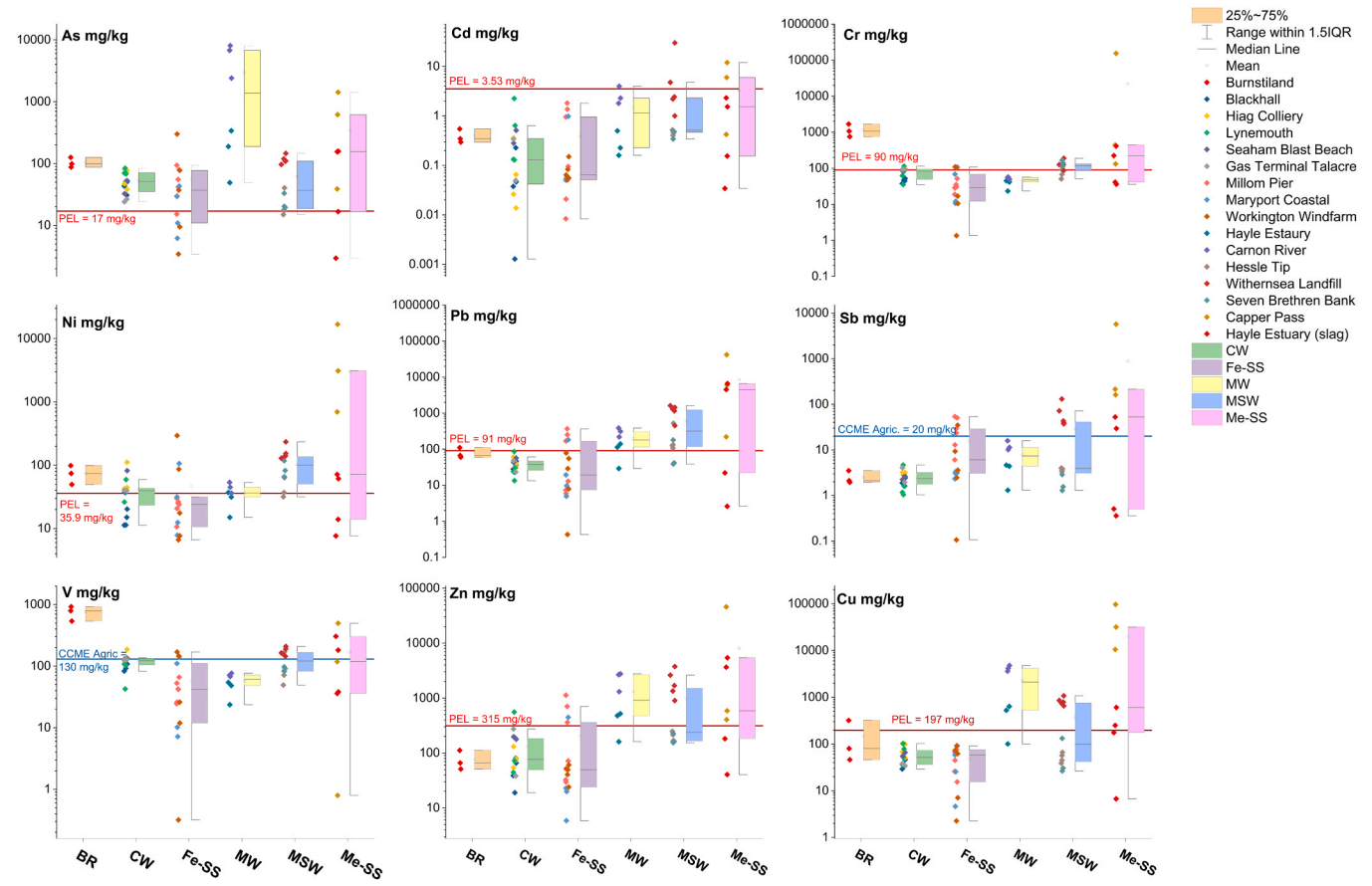

Fig. 3. Potential toxic element concentrations box plots for each waste type and sites. BR: Bauxite residues; CW: colliery waste; Fe-SS: ferrous and steel slags; MW: mining waste; MSW: municipal solid wastes; Me-SS: non-ferrous slags. Red lines indicate the predicted effect level (PEL) for adverse conditions to the ecosystem; Blue lines, for Sb and V, refer to the threshold for agricultural land [42,46]

crust (Figure S.1). Chromium concentration medians were highest for the BR (1070 mg kg^{-1}) and Me-SS samples (220 mg kg^{-1}); the latter also had the largest Cr concentration range (36 – 153700 mg kg^{-1}) and highest Cr enrichment relative to upper continental crust (Figure S.1). The Cr median concentration for the MSW samples was 1120 mg kg^{-1} and the CW, Fe-SS, and MW samples had the lowest Cr concentrations.

All Cu concentrations of the Me-SS, MW, and MSW samples were enriched compared to those of the upper continental crust (Figure S.1). The Me-SS and MW samples had the highest Cu concentrations (median 2120 and 20000 mg kg^{-1}, respectively) (Fig. 3). The median Cu concentrations of other waste type samples were < 100 mg kg^{-1}, although MSW maximum values reached 96700 mg kg^{-1} for Withernsea samples (Fig. 3). Median Ni concentrations of the CW, Fe-SS, and MW samples ranged between 20 and 40 mg kg^{-1}. By contrast, the median Ni concentration of the Me-SS samples was 70 mg kg^{-1}; these samples also had a large Ni concentration range (8 – 16870 mg kg^{-1}). The MSW samples had the highest median Ni concentrations (100 mg kg^{-1}) followed by the BR samples (74 mg kg^{-1}).

Lead median concentrations were highest for Me-SS (4500 mg kg^{-1}) and MSW (320 mg kg^{-1}), followed by MW (180 mg kg^{-1}) (Fig. 3, Figure S.1). Median Pb concentrations of the CW, Fe-SS and BR samples were < 40, 20 and 70 mg kg^{-1}, respectively. The Sb median concentration was high for Me-SS (50 mg kg^{-1}) and all the other Sb medians were lower than 10 mg kg^{-1}, although they were enriched compared to upper continental crust concentrations (Figure S.1). High concentration variability was notable for Me-SS, Fe-SS, and MSW (Fig. 3). BR samples had the highest V concentrations (median 540 mg kg^{-1}) and CW, MSW, and Me-SS had V medians around 120 mg kg^{-1}. Fe-SS and MW V median concentrations were the lowest (40 and 60 mg kg^{-1}, respectively). Zinc median concentrations were high for Me-SS (590 mg kg^{-1}), MW (910 mg kg^{-1}), and MSW (240 mg kg^{-1}). Other wastes had medians lower than 100 mg kg^{-1} Zn that were similar to the upper crust Zn concentration (Fig. 3, Figure S.1).

4. Discussion

4.1. Mineralogy and geochemistry of legacy wastes

4.1.1. Colliery waste

Generally, Colliery waste (CW) samples mostly had consistent bulk chemical compositions across sites (Figure S.1) and mineralogy typical of this type of waste [47] that was dominated by quartz, kaolinite, illite, and plagioclase (Table 1). Major elemental concentrations were similar to values reported in other studies [48] with Si, Fe, and Al dominating (Table S2.a). The mineralogy reflected major element concentration variations across the different sites, with samples from Haig Colliery enriched in Al, K, and Na, probably due the presence of abundant feldspars. High Fe concentrations were either due to pyrite and pyrite-clay mixed phases (Lynemouth) or Fe-oxide and chlorite (Haig Colliery) (Table 2. In the Haig Colliery and Black Hall samples, the presence of mullite, magnetite, and high-temperature phase sanidine (Table 2) suggested that the primary minerals had been heated.

PTE concentrations can vary due to the differences within the formation environment, and post-depositional and anthropogenic biogeochemical processes [47]. Arsenic concentrations in the CW were above predicted effect levels (PEL) (CCME, 2001) and V concentrations were just below the guideline value (agricultural land, Agric) CCME, 2011) (Fig. 3). Arsenic concentrations were similar to those recorded in UK

ferrous mineralisation and coal mining areas (mean 73 mg kg^{-1}) [45]. The sites having the highest As concentrations were Lynemouth and Haig Colliery. At Lynemouth, the As-, Cu-, and Zn-bearing minerals were mostly pyrite and secondary sulfates. Vanadium may be associated with oxides, or as observed in other studies, to clay minerals and organic matter [49,50].

4.1.2. Mining wastes

Mining waste (MW) samples from Hayle Estuary and Restronguet Creek had no significant differences in major element concentrations, with the exception of Mg ($p < 0.05$) (Table S2.b). Calcium concentrations and carbonate minerals were more abundant in the Hayle Estuary samples (Table 1). PTE-bearing minerals varied across sites, with the Restronguet Creek samples containing 0.5 vol% As- and Cu- bearing scorodite, bukovskyite, and chalcopyrite, and the Hayle Estuary, Pb and Zn-bearing Fe- and Al-oxides, and occasionally As-bearing pyrite (Table 2; Fig. 2, and Fig. 3). Both areas showed high PTE concentrations similar to those reported in other UK areas [51] and other MW in Europe [52] (Tables S2.b and S3).

MW exhibited the highest arsenic (As) concentrations among the analysed waste types, with values reaching up to 8000 % above the Probable Effect Level (PEL). In comparison, median As concentrations in UK topsoils are generally lower (46 mg/kg; [45]). However, studies conducted in Cornish estuaries also reported elevated mine waste As concentrations [38,53]. Median concentrations of Cu and Pb in MW also exceeded both PEL thresholds and typical values for UK urban and mineralised topsoils (Fig. 3; Table S2.b) [45]. Lead was identified in multiple mineral phases, including sulfides (galena), sulfates (anglesite), carbonates (cerussite), and phosphates (plumbogummite) (Table 2).

4.1.3. Ferrous slags

The presence of melilite (gehlenite and åkermanite), pyroxene (hedenbergite), and olivine (monticellite) indicated Si and Ca-rich smelting waste (Table 2; Table S2.c), typical of Fe-SS [11,54]. Carbonate (calcite and ankerite) and sulfates (gypsum and Fe sulfates) were likely secondary minerals forming from the weathering of the previous minerals (Tables 1, and 2). The observed lime may have been the residue of flux materials. Glass material with a Si-Ca-Al-Mn-O composition and likely formed due to fast cooling was found in the Workington Windfarm samples. The enriched Fe median concentrations (10 wt%) suggested that Fe was not efficiently processed during the smelting process. Indeed, variations among the Fe-SS wastes may be due to their different ore mineralogy, methods of extraction, and processing histories [11,55].

Maryport Coastal and Workington Windfarm samples occasionally presented major elements and mineralogical compositions similar to CW, low Ca and C concentrations and low temperature minerals (quartz, feldspar, illite, kaolinite, with additional Fe-oxides). This may indicate the disposal of different waste in formal slag waste areas. For example, coke (and associated ashes) used in the production of iron and steel [56] and wastes from nearby collieries may be co-disposed at some of the locations (e.g. [11]).

PTE medians were generally higher than the concentrations reported by Piatak et al. [39] (Table S2.c) but were in agreement with those described by Riley et al. [11], who focused on UK Fe-SS wastes. The As average (60 mg kg-1) was almost tenfold higher than the literature average (7 mg kg^{-1}; [39]) and higher than PEL values (Fig. 3). This is potentially due to Fe-SS - CW co-disposal and rich As-bearing Fe – S mineral phases. Also, Ni concentrations were occasionally 300 % higher than PEL values and held in Ca – O phases.

4.1.4. Non-ferrous slags

Three types of Me-SSs were recognised: Cr-enriched slag associated with Sb and V, Zn-enriched slag, and Cu enriched slag associated with Ni- and Pb-rich metal droplets and minerals. Me-SS major chemistry was in line with findings from Piatak et al. [39] (Table S2.d). Generally, Cr and Ni concentrations were higher than literature concentrations and the other PTEs were within the literature ranges and towards the lower part (Table S2.d). Only Cd showed generally lower concentrations (average 3 mg kg^{-1}) than those (541 mg kg^{-1}) reported by Piatak et al. [39] for Zn, Pb, and Cu slags.

PTE concentrations were generally above the PEL and AGRIC guidelines (CCME, 2001), except for Cd, which had a median concentration below the PEL threshold (3.5 mg kg^{-1}) and only a few samples exceeding this value (Fig. 3). A variety of minerals hosted PTEs (Table 2). In line with previous studies (e.g., Piatek et al., 2015 and references therein), spinels with the general formula AB_2O_4 were found to incorporate Zn, Mn, and Mg as divalent A-site ions and Al, Fe, or Cr as trivalent B-site ions—examples include magnesioferrite, jacobsite, Mg-aluminate, and Cr-spinel (Table 2).

In samples from Capper Pass Ni was associated with Sn and Cu in potential alloy phases and fayalite-like structures (O–Mg–Si–Fe–Ni), often co-occurring with Cr and Cu. Similar mineral assemblages, including Cr-rich spinel and olivine, have been documented in historical Cu slags from Kazakhstan [57]. Cassiterite (SnO_2) and Cu–Sn–O phases were identified as Sb hosts. Copper was present as metallic droplets—often with Pb, Sn, and Ni—as well as in Cu sulfides (e.g., covellite, chalcocite, chalcopyrite) and oxides such as paramelaconite (Cu_4O_3).

4.1.5. Municipal solid wastes

MSW mineral associations were similar to those reported for bottom ashes, and were dominated by quartz, calcite, feldspars, sulfates, chloride, and iron hydroxide [12] (Table 1). However, bottom ashes also contained amorphous material, micro-structure inclusions, and high-temperature minerals such as pyroxene and gehlenite-åkermanite [12,58]. In this study, the dominant minerals (23 vol% of total) were Fe-oxides (often mixed with Al, Mn, and carbonate) (Tables 1 and 2), either formed during the ageing oxidative phases [59] or uncontrolled burning events typical of legacy MSW.

Major and PTE concentration medians from different MSW material and impacted sediments were in accordance with literature data (Table S2.e) [5,60]. Significant variability among sites may be due to the origin and age of waste discarded into the landfill [61]. As an example, Hessle Tip was mostly formed by construction waste and had a high calcite and Ca concentrations.

PTE concentrations varied up to two orders of magnitude among sites (Fig. 3), in accordance with results reported by Brand et al. [5], and were mostly contained in Fe-oxides (Table 2). Generally, As, Cr, Ni, and Pb concentrations were higher than PEL values. Nickel and Cr-bearing minerals were not found, potentially indicating low Ni and Cr absorption onto Fe hydro-oxides and clay minerals [62]. Arsenic, herein associated with pyrite and metal (including Fe) oxides (Table 2), may originate from different sources, such as the co-disposal of coal wastes, glass, pigments, textiles, paper, and wood preservatives [63,64].

MSW had high Pb concentrations hosted in various minerals, sulfate (barite, Pb-sulfate), titanite, and oxide minerals (Table 2). Barite and Pb potentially originated from incinerated paint [65]. The Pb concentrations were in line with those of UK topsoil in urban areas (320 mg kg^{-1}; [45]) and below high range concentrations observed at Thames Estuary landfill sites (Hadleigh Marsh landfill, 3620–4830 mg kg^{-1}; [66]). At Withernsea Pb sources such as textiles and paper were difficult to recognise since most of the material went through combustion. Other potential Pb sources were obsolete and weathered electronic material, as observed at Seven Brethren Bank.

Concentrations of PTEs such as Cu, Zn, Cd, Sb, and V were generally below the PEL and AGRIC guideline values, except in samples from the Withernsea site. Copper was commonly found as metal alloys or within Cu–Fe–O and Cu–Fe–S phases, likely representing Cu-bearing iron oxides and sulfides (Table 2). In historical MSW landfills, elevated Cu concentrations have been identified in the sediment matrix as well as in textile and paper wastes [14]. Aged incinerated MSW residues also contained Ni and Cu associated with Fe oxides and carbonates [58].

Similarly, Cu-sulfide minerals and Cu-bearing Fe oxides have been reported in bottom ashes from modern incineration plants in Germany and the Netherlands [58,65].

At Withernsea, Zn-bearing phases included silicates and iron oxides (Table 2; Fig. 2). Zn concentrations observed here were comparable to those in German incinerated MSW, where approximately 20 % of the total Zn was acid-extractable, likely due to the dissolution of carbonates and oxides [60]. While no Zn-carbonate minerals were directly identified in this study, carbonate phases were ubiquitous across sites, and low-level Zn sorption (below analytical detection limits) may have occurred.

Information on Sb and V geochemistry in MSW remained limited. William et al. [61] reported Sb concentrations lower than those observed in this study (Table S2.e). Antimony could enter the MSW via oxides used in flame retardants, lead-acid batteries, textiles, and plastics [67]. Vanadium, detected at relatively low levels, was likely of lithogenic origin, with background concentrations ranging from 22 to 118 mg kg^{-1} , similar to those reported by [3].

4.1.6. *Bauxite residues*

BR mineralogy and major element concentrations (Table 1 and Table S2.f) were consistent with those of BR studied in other areas [68-70]. Arsenic, Cr, and V concentrations were 5–6 times higher than PEL values (Fig. 3), although no PTE bearing minerals were observed during the mineralogical analysis. This aligns with findings from the Ajka alumina plant in western Hungary, where no As-bearing minerals were detected in the BR despite a mean As concentration of 200 mg kg^{-1} . In that case, As was primarily present in a mobile form (arsenate), with its mobility influenced by pH and redox conditions [71]. The elevated V BR concentrations were in agreement with the BR literature, where V recovery has been extensively studied [72,73].

4.2. *PTE in legacy wastes and potential ecosystem exposure*

Coastal erosion and seawater inundation can increase PTE concentrations in the pore water and water column in seawaters or transitional water [15]. Legacy wastes, as identified here and in Riley et al. [11], are only partially protected by coastal defences and often exhibit signs of erosion and contaminant transfer. Following seawater inundation, wastes are subject to variations in pH, Eh, and salinity. Prolonged seawater inundation may promote reducing conditions, generating instability of PTE absorbed onto organic matter, Fe and Mn oxides and sulfate (Lyden et al., 2022). Furthermore, low Fe concentrated seawaters can trigger Fe-bearing mineral dissolution in freshwater sediment and waste [16,74]. Mineralogical information is critical to help predict potential PTE release mechanisms in coastal areas where dissolution and PTE release are driven by reaction kinetics and microorganism presence. The mineralogical and PTE information obtained in this study for legacy wastes along the UK coast is used in this section to summarise the potential hazards and contaminant release mechanisms in different waste types (Fig. 4).

Coastal and transitional waters undergo complex chemical transformations due to the dynamic interaction of fresh and saline water in both surface and subsurface environments. Climate change will exacerbate coastal flooding in the UK by increasing sea level by as much as 80 cm by 2100, depending on projection scenarios [75], and by causing increases and decreases in winter and summer river flows, respectively.

4.2.1. *Coal wastes*

In CW, PTEs were associated with primary minerals such as sulfides and secondary minerals (Fe-oxides, sulfate, clay and mica) (Table 2, Fig. 4). The presence of gypsum and jarosite (Table 2) indicated weathering of sulfides and mineral precipitation from Ca^{2+}- and SO_4^{2-}-enriched percolating waters [48]. Sulfide weathering generated a drop in pH, as observed in leaching studies [76], enhancing PTE-bearing Fe-sulfates precipitation. PTE had less mobility and stayed stable until the occurrence of geochemical variations (pH, Eh, or salinity) [16].

Leaching experiments on CW legacy wastes under deionised- and seawaters have demonstrated PTE release variability among and within waste sites, with potential As release up to around 10 % of total As [76]. In weathering oxidising conditions, mobility of As could be linked to the dissolution of sulfides (such as pyrite and arsenopyrite) [77] or by high surface area minerals, such as clay and mica [76]. Under reducing conditions typical of prolonged seawater flooding, other PTEs, namely Zn and Cu, could be released by Fe and Mn oxides (including hydroxides and oxyhydroxides) [76] and poorly crystalline sulfate, such as jarosite [15]. In addition, the organic matter, highest in the CW compared to the other wastes (Table S2.a) and with a potential affinity with PTE [78], could be the first to be reduced and release PTE. Finally, under seawater inundation, Cl-complexes and cation exchange between the seawater cations and the PTE-bearing minerals could enhance PTE mobility (Fig. 4) [15].

In coastal environments, where either reducing or oxidising conditions can occur depending on seasonality, extreme events, and coastal

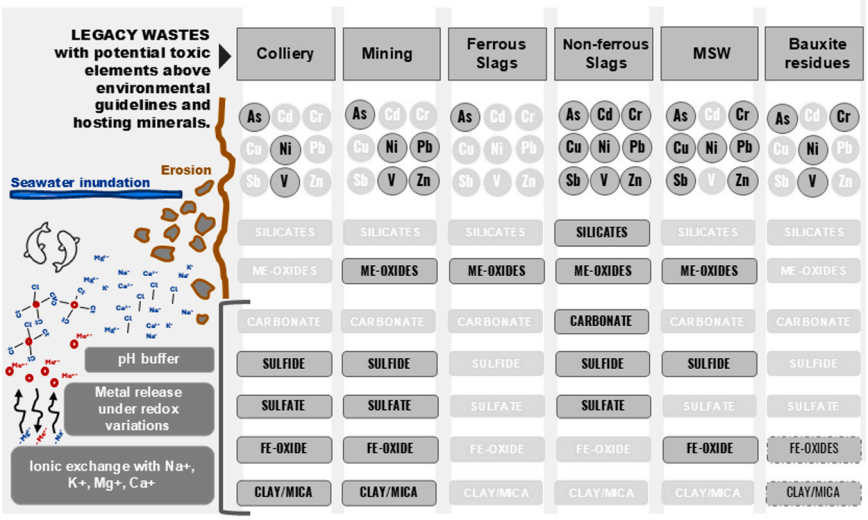

Fig. 4. Summary of potential hazards posed by colliery, mining, ferrous and non-ferrous slag and bauxite waste types. The boxes highlighted in black and grey show the median PTE above the environmental threshold, which may pose adverse effects to the ecosystem and the PTE-bearing minerals. The bottom minerals are the most likely to release metals under seawater inundation conditions. On the left, the major reactions occurring under seawater inundations are reported.

physical erosion, CW, comprising around 40 vol% of PTE-bearing minerals (Table 1, Fig. 4), may show high reactivity and release PTE into the ecosystem. Therefore, CW could pose a hazard to the environment, especially with respect to As concentrations (Fig. 2), and occasionally other PTE, if not correctly characterised and managed.

4.2.2. Mining wastes

PTE-bearing minerals in MW had similarities with those held in CW (sulfides, sulfates, Fe-oxides, and clay) plus some other trace minerals, such as carbonates (cerussite), and phosphate (plumbogummite) (Table 2, Fig. 3). MW were rich in PTE, with six elements out of the nine investigated, above environmental threshold limits (Figs. 3 and 4). The mineralogy suggested PTE mobility mechanisms [79], with Pb, Cu, and Zn being initially released by sulfide minerals and then taken up by carbonate and phosphate phases, Fe-oxide minerals, and clays (Table 2).

Legacy MW in coastal areas had around 45 vol% of potentially reactive minerals (Table 1, Fig. 4) that can easily further release PTE into the ecosystem due to redox, pH, streamflow variations, and storm events. MW impacts on estuaries were flagged under the 1992 Oslo Paris Convention [80], which linked Zn, Cu, Pb, and Cd concentrations in estuarine areas to fluxes from mining-impacted river catchments. Most legacy MW is transported and deposited in catchment and the estuarine areas [81,82]. The huge volumes of legacy MW that reside within riverine and estuarine systems can be mobilised physically or release PTE in colloidal and dissolved form [40,53,83].

4.2.3. Municipal solid wastes

MSW contained an average of 10 vol% PTE-bearing Fe oxides (Table 1) that can release PTE under acidic or reducing conditions during flooding or sediment transportation. Lead, Zn, Cr, and As were associated with Fe oxide or Pb oxide phases (Table 2). At WS, Pb oxides potentially originated from the disposal of waste, such as paint, or formed during waste combustion when the initial mineralogy and metal mobility was altered [84]. Organic matter concentrations, which may reach 20 wt% as organic carbon as at Withernsea (Figure S.2), can enhance Pb-oxide weathering [85]. Similar to CW, other PTE sources could be sulfides (such as galena, sphalerite, and pyrite) that under oxidative conditions could release Fe, Zn, Pb, and As (Table 2) [79]. However, the MSW sulfide content was < 1 vol% (Table 1) suggesting that this is not an important process in the studied sites.

PTE leachability studies have indicated potential dispersion mechanisms, although these are limited by scant associated mineralogical investigations. Lead was highlighted as a highly mobility PTE at Hadleigh Marsh legacy MSW especially under freshwater conditions [5]. Other PTEs, such as Zn and Cd were found to be more mobile in seawater [5,86]. Leaching of incinerated MSW showed that the majority of Ni was not mobile [60] and in legacy MSW, Ni leaching was limited to < 1 %, with slightly higher values in the case of seawater leaching (Brand et al., 2020). Potential release and dispersion of Cu has been suggested to occur through physical erosion (Brand et al., 2019) and fresh- or seawater leaching [87]. PTEs could also be found as insoluble precipitates or strongly absorbed species, limiting their release to particle dispersion under erosive events [17]. Overall, the MSW mineralogy and literature studies on PTE leaching experiments indicated potential PTE release under freshwater and seawater conditions, potentially posing a risk to the environment.

4.2.4. Ferrous and metal slag wastes

Fe-SS had low PTE concentrations except for As occasionally showing concentrations higher than PEL values (Fig. 3). Elevated As concentrations may be due to the disposal of CW within Fe-SS deposits, as highlighted by the mineralogical and chemical results (Fig. 3, Table 2). Previous studies involving similar locations to those investigated (Table S1) showed low amounts of PTE leaching under fresh- and seawater conditions, with Cr and V mostly in their less mobile species, V^{3+} and Cr^{3+}, and associated with low solubility minerals such as spinels [11].

Me-SS showed higher mean PTE mean concentrations than those of PEL (up to 800 %) associated with olivine, sorosilicates, sulfides, spinels, and other oxides (Table 2, Fig. 4). Olivine, sorosilicates, and spinels, bearing Cr, Cu, Ni, Pb, and V have been known in the literature for their low solubility potentially limiting PTE mobility under various environmental conditions [88]. In the Cr-jacobsite spinel, Cr was likely held in the less mobile species, Cr(III), although oxidation to Cr(VI) could occur in the presence of Mn oxides [89,90] observed in association with Cr-bearing mineral (Table 2). Me-SS also had metal phases such as Pb metal droplet smelting residues with limited metal mobility.

In Me-SS, PTE release into the water and sediment may occur due to sulfide weathering under oxidising conditions, but there was little evidence of this (Fig. 4; Tables 1 and 2). However, caution should be taken when managing Me-SS waste, due to their high concentrations of PTE that could be released under direct receptor contact, such as soil, sediment-dwelling organisms, and accelerated bio-weathering processes [91].

4.2.5. Bauxite residues

Bauxite residues can pose an environmental risk due to PTE concentrations higher than PEL values, such as As (around 100 mg kg^{-1}), Ni (70 mg kg^{-1}), Cr and V (around 1000 mg kg^{-1}) (Fig. 4 and Table S2.f). The mobility of PTE from BR has been shown to be pH dependent and controlled by sorption to mineral surfaces [92]. Under circumneutral pH, As mobility is dominated by adsorption processes, whereas V and especially Cr mobility increases in their oxyanion form at high pH [92,93]. Circumneutral to alkaline conditions would occur during seawater inundation or Ca- and Na-rich aluminate and hydroxides weathering (Table 2) [92,93]. Furthermore, seawater cations could compete with As sorption and enhance its mobility into the water column [94].

5. Conclusions and recommendations for management and future research

Elevated concentrations of PTEs were present in representative UK coastal legacy wastes that have the potential for geochemical release mechanisms into the coastal environment. The findings indicate that, except for the ferrous slags, all the investigated waste types pose a potential risk for PTE contamination, reinforcing the need for stringent monitoring and management strategies. Colliery wastes, mining, and municipal solid wastes have the highest potential for PTE mobility given the ubiquity of secondary minerals forming at the expense of primary unstable PTE-bearing minerals. Metal smelting slags had the highest PTE concentrations, although these were present in silicates, metals (droplets), and oxides such as spinel and rutile groups that have low solubilities under environmental conditions. Legacy waste mineralogy provides crucial information for predicting PET dispersion under prolonged flooding and coastal erosion, or during remediation efforts. This underscores the need to thoroughly characterise the mineralogy of legacy wastes, especially considering that some materials may originate from different sources, such as co-disposed wastes.

PTEs concentrations reported in this research highlight the variability among and within legacy wastes and demonstrate that reliance solely on elemental bulk analysis may not fully capture the complexities of elemental dispersion. Leaching experiments are fundamental for determining potential release processes in legacy wastes and further efforts in this direction are encouraged. The findings here contribute valuable insights into the management of PTE-bearing minerals in both freshwater and seawater environments.

Our study focussed on characterisation of inorganic contaminants only and did not evaluate leachability under seawater inundation. Although our sampling covered multiple waste types and locations throughout the UK, the conclusions are inherently grounded in this national setting and may not fully reflect differing geological, hydrological or management conditions elsewhere. However, the

comprehensive mineralogical and geochemical dataset in this study could be integrated into national prioritisation schemes to monitor and reduce contamination risks. As highlighted by previous studies (Brand et al., 2020; [76]), understanding waste heterogeneity is critical when planning monitoring programs and careful sampling strategies to avoid destabilisation and erosion [5]. Therefore, this robust dataset can facilitate cost-effective interventions by providing comparative data for different waste types. By integrating mineralogical and geochemical data with information on waste location and volume, regulators can enhance their environmental management strategies.

Environmental Implications

Coastal legacy wastes are enriched in potentially toxic elements (PTEs), with unique mineral associations that control their stability and release. Mineralogical characterisation is therefore essential to predict contaminant pathways under environmentally relevant conditions. Our study suggests that seawater inundation, coastal erosion, and redox shifts can destabilise PTE-bearing minerals, enhancing PTE mobility. Coal and mining wastes present the greatest risks due to their abundance of soluble and redox-sensitive secondary minerals. These findings provide a strong scientific basis for improved monitoring, risk assessment, and remediation strategies, supporting protection of coastal ecosystems and human health under climate change pressures.

CRediT authorship contribution statement

Will M. Mayes: Writing – review & editing, Resources, Methodology, Investigation, Funding acquisition, Conceptualization. **Adam P. Jarvis:** Writing – review & editing, Resources, Methodology, Investigation, Funding acquisition, Conceptualization. **Bryan M. Spears:** Writing – review & editing, Investigation. **Justyna P. Olszewska:** Writing – review & editing, Investigation. **Gavyn K. Rollison:** Writing – review & editing, Methodology, Formal analysis, Data curation. **Patrick Byrne:** Writing – review & editing, Visualization, Investigation. **Rich A. Crane:** Writing – review & editing, Methodology, Investigation. **Ian T. Burke:** Writing – review & editing, Visualization, Methodology, Conceptualization. **Karen Hudson-Edwards:** Writing – original draft, Resources, Methodology, Investigation, Funding acquisition, Conceptualization, Writing – review & editing. **Alex L. Riley:** Writing – review & editing, Visualization, Investigation, Formal analysis. **Catherine J. Gandy:** Writing – review & editing, Investigation. **Elin Jennings:** Writing – review & editing, Methodology, Investigation, Formal analysis, Data curation. **Violeta Ramos:** Writing – original draft, Methodology, Investigation, Formal analysis, Data curation. **Patrizia Onnis:** Writing – original draft, Visualization, Methodology, Investigation, Formal analysis, Data curation, Conceptualization, Writing – review & editing.

Declaration of Competing Interest

The authors declare the following financial interests/personal relationships which may be considered as potential competing interests: Will Mayes, Adam Jarvis, Karen Hudson-Edwards reports financial support was provided by UK Research and Innovation Natural Environment Research Council. If there are other authors, they declare that they have no known competing financial interests or personal relationships that could have appeared to influence the work reported in this paper.

Acknowledgements

This work was supported by the Natural Environment Research Council (NERC) under grant numbers NE/T003022/1, NE/T003200/1, NE/T003286/1 and NE/T002824/1. The authors thank Natural Resources Wales and the Environment Agency for their assistance with site access, and Sharon Uren for her support with sample analysis.

Appendix A. Supporting information

Supplementary data associated with this article can be found in the online version at doi:10.1016/j.jhazmat.2026.141180.

Data availability

Data will be made available on request.

References

[1] Cooper, N., Bower, G., Tyson, R., Flikweert, J., Rayner, S. Hallas, A. 2013. Guidance on the management of landfill sites and land contamination on eroding or low-lying coastlines. CIRIA, C718, London.
[2] Irfan, M., Houdayer, B., Shah, H., Koj, A., Thomas, H., 2019. GIS-based investigation of historic landfill sites in the coastal zones of Wales (UK). EurMediterr J Environ Integr 4, 26. https://doi.org/10.1007/s41207-019-0116-y.
[3] O'Shea, F.T., Cundy, A.B., Spencer, K.L., 2018. The contaminant legacy from historic coastal landfills and their potential as sources of diffuse pollution. Mar Pollut Bull 128, 446–455. https://doi.org/10.1016/j.marpolbul.2017.12.047.
[4] Shukla, O.P., Rai, U.N., 2009. Natural attenuation: A potential for environmental cleanup. ⟨http://isebindia.com/09-12/09-04-3.html⟩ (Accessed 29 August 2024).
[5] Brand, J.H., Spencer, K.L., O'Shea, F.T., Lindsay, J.E., 2018. Potential pollution risks of historic landfills on low-lying coasts and estuaries. WIREs Water 5, e1264. https://doi.org/10.1002/wat2.1264.
[6] Neuhold, C., Nachtnebel, H.P., 2011. Assessing flood risk associated with waste disposals: methodology, application and uncertainties. Nat Hazards 56, 359–370. https://doi.org/10.1007/s11069-010-9575-9.
[7] Kim, N.D., Taylor, M.D., Caldwell, J., Rumsby, A., Champeau, O., Tremblay, L.A., 2020. Development and deployment of a framework to prioritise environmental contamination issues. Sustainability 12, 9393. https://doi.org/10.3390/su12229393.
[8] Ouyang, K., Lu, X., Meng, J., Wang, C., Feng, S., Shi, B., et al., 2024. Which pollutants and sources should be prioritised for control in multi-pollutants complex contaminated areas? J Hazard Mater 478, 135547. https://doi.org/10.1016/j.jhazmat.2024.135547.
[9] Riley, A.L., Amezaga, J., Burke, I.T., Byrne, P., Cooper, N., Crane, R.A., et al., 2022. Incorporating conceptual site models into national-scale environmental risk assessments for legacy waste in the coastal zone. Front Environ Sci 10, 1045482. https://doi.org/10.3389/fenvs.2022.1045482.
[10] Lee, G., Jun, K.S., Kang, M., 2019. Framework to prioritize watersheds for diffuse pollution management in the Republic of Korea: application of multi-criteria analysis using the Delphi method. Nat. Hazards Earth Syst. Sci. 19, 2767–2779. https://doi.org/10.5194/nhess-19-2767-2019.
[11] Riley, A.L., Cameron, J., Burke, I.T., Onnis, P., MacDonald, J.M., Gandy, C.J., et al., 2024. Environmental behaviour of iron and steel slags in coastal settings. Environ Sci Pollut R. https://doi.org/10.1007/s11356-024-33897-4.
[12] Mantovani, L., De Matteis, C., Tribaudino, M., Boschetti, T., Funari, V., Dinelli, E., et al., 2023. Grain size and mineralogical constraints on leaching in the bottom ashes from municipal solid waste incineration: a comparison of five plants in northern Italy. Front Environ Sci 11, 1179272. https://doi.org/10.3389/fenvs.2023.1179272.
[13] Saxena, P., Song, X., Zhang, B., Sarkar, A., Achari, G., 2025. Profiling PBDE emissions from coastal landfills: Impact of waste management practices. Waste Manag Bull 3, 391–401. https://doi.org/10.1016/j.wmb.2025.02.005.
[14] Brand, J.H., Spencer, K.L., 2019. Potential contamination of the coastal zone by eroding historic landfills. Mar. Pollut. Bull. 146, 282–291. https://doi.org/10.1016/j.marpolbul.2019.06.017.
[15] Du Laing, G., Rinklebe, J., Vandecasteele, B., Meers, E., Tack, F.M.G., 2009. Trace metal behaviour in estuarine and riverine floodplain soils and sediments: a review. Sci Total Environ 407, 3972–3985. https://doi.org/10.1016/j.scitotenv.2008.07.025.
[16] Leyden, E., Farkas, J., Hutson, J., Mosley, L.M., 2022. Short-term seawater inundation induces metal mobilisation in freshwater and acid sulfate soil environments. Chemosphere 299, 134383. https://doi.org/10.1016/j.chemosphere.2022.134383.
[17] Burke, I.T., Onnis, P., Riley, A.L., Gandy, C.J., Ramos, V., Rollinson, G.K., et al., 2025. Speciation and leaching behaviour of inorganic contaminants in actively eroding historical coastal municipal solid waste landfills. Mar Pollut Bull 219, 118341. https://doi.org/10.1016/j.marpolbul.2025.118341.
[18] de Souza Machado, A.A., Spencer, K., Kloas, W., Toffolon, M., Zarfl, C., 2016. Metal fate and effects in estuaries: a review and conceptual model for better understanding of toxicity. Sci Total Environ 541, 268–281. https://doi.org/10.1016/j.scitotenv.2015.09.045.
[19] Nordstrom, D.K., 2011. Hydrogeochemical processes governing the origin, transport and fate of major and trace elements from mine wastes and mineralised rock to surface waters. Appl Geochem 26, 1777–1791. https://doi.org/10.1016/j.apgeochem.2011.06.002.

[20] Chung, J.-Y., Yu, S.-D., Hong, Y.-S., 2014. Environmental source of arsenic exposure. J Prev Med Public Health 47, 253–257. https://doi.org/10.3961/jpmph.14.036.
[21] Patel, K.S., Pandey, P.K., Martín-Ramos, P., Corns, W.T., Varol, S., Bhattacharya, P., et al., 2023. A review on arsenic in the environment: contamination, mobility, sources, and exposure. RSC Adv 13, 8803. https://doi.org/10.1039/d3ra00789h.
[22] Cheng, K., Tian, H., Zhao, D., Lu, L., Wang, Y., Chen, J., et al., 2014. Atmospheric emission inventory of cadmium from anthropogenic sources. Int J Environ Sci Technol 11, 605–616. https://doi.org/10.1007/s13762-013-0206-3.
[23] Costa, M., Klein, C.B., 2006. Toxicity and carcinogenicity of chromium compounds in humans. Crc Rev Toxicol 36, 155–163. https://doi.org/10.1080/10408440500534032.
[24] Kimbrough, K.L., Commey, S., Apetia, D.A., Lauensteina, G.G., 2010. Chemical contamination assessment of the Hudson–Raritan Estuary as a result of the attacks on the World Trade Center: analysis of trace elements. Mar Pollut Bull 60, 2289–2296. https://doi.org/10.1016/j.marpolbul.2010.07.009.
[25] Wnuk, E., 2023. Mobility, bioavailability, and toxicity of vanadium regulated by physicochemical and biological properties of the soil. J Soil Sci Plant Nut 23, 1386–1396. https://doi.org/10.1007/s42729-023-01130-9.
[26] Bolan, N., Kunhikrishnan, A., Thangarajan, R., Kumpiene, J., Park, J., Makino, T., et al., 2014. Remediation of heavy metal(loid)s contaminated soils - to mobilise or to immobilise? J Hazard Mater 266, 141–166. https://doi.org/10.1016/j.jhazmat.2013.12.018.
[27] Chandrangsu, P., Rensing, C., Helmann, J.D., 2017. Metal homeostasis and resistance in bacteria. Nat Rev Microbiol 15, 338–350. https://doi.org/10.1038/nrmicro.2017.15.
[28] Genchi, G., Sinicropi, M.S., Lauria, G., Carocci, A., Catalano, A., 2020. The effects of cadmium toxicity. Int J Environ Res Public Health 26, 3782. https://doi.org/10.3390/ijerph17113782.
[29] Kulp, S.A., Strauss, B.H., 2019. New elevation data triple estimates of global vulnerability to sea-level rise and coastal flooding. Nat Commun 10, 4844. https://doi.org/10.1038/s41467-019-12808-z.
[30] Neubauer, S.C., Franklin, R.B., Berrier, D.J., 2013. Saltwater intrusion into tidal freshwater marshes alters the biogeochemical processing of organic carbon. Biogeosciences 10, 8171–8183. https://doi.org/10.5194/bg-10-8171-2013, 2013.
[31] Marchuk, A., Rengasamy, P., 2011. Clay behaviour in suspension is related to the ionicity of clay–cation bonds. Appl Clay Sci 53, 754–759. https://doi.org/10.1016/j.clay.2011.05.019.
[32] Miranda, L.S., Ayoko, G.A., Egodawatta, P., Goonetilleke, A., 2022. Adsorption-desorption behavior of heavy metals in aquatic environments: influence of sediment, water and metal ionic properties. J Hazard Mater 421, 126743. https://doi.org/10.1016/j.jhazmat.2021.126743.
[33] Acosta, J.A., Jansen, B., Kalbitz, K., Faz, A., Martínez-Martínez, S., 2011. Salinity increases mobility of heavy metals in soils. Chemosphere 85, 1318–1324. https://doi.org/10.1016/j.chemosphere.2011.07.046.
[34] Moore, W.S., Joye, S.B., 2021. Saltwater intrusion and submarine groundwater discharge: acceleration of biogeochemical reactions in changing coastal aquifers. Front Earth Sci 9, 600710. https://doi.org/10.3389/feart.2021.600710.
[35] Brand, J.H., Spencer, K.L., 2020. Will flooding or erosion of historic landfills result in a significant release of soluble contaminants to the coastal zone? Sci. Total Environ. 724, 138150. https://doi.org/10.1016/j.scitotenv.2020.138150.
[36] Nicholls, R.J., Beaven, R.P., Stringfellow, A., Monfort, D., Le Cozannet, G., Wahl, T., et al., 2021. Coastal landfills and rising sea Levels: a challenge for the 21st Century. Front Mar Sci 8, 710342. https://doi.org/10.3389/fmars.2021.710342.
[37] Onnis, P., Riley, A. L., Gandy, C. E., JenningsE., Crane, R.A., Byrne, P., Rollinson, G., Jarvis, A. P., Mayes, W. M., Hudson-Edwards, K.A. Coastal wastes geochemistry and mineralogy as a tool to identify potential metal(loid) sources. In Edraki, M, Jones, D., and Jain, K.R. (eds) Proceedings of the Twelfth International Conference on Acid Rock Drainage, online. 18-24 September 2022.pp. 894-905 (The University of Queensland: Brisbane).
[38] Rollinson, G.K., Andersen, J.C.Ø., Stickland, R.J., Boni, M., Fairhurst, R., 2011. Characterisation of non-sulphide Zn deposits using QEMSCAN®. Miner Eng 24, 778–787. https://doi.org/10.1016/j.mineng.2011.02.004.
[39] Piatak, N.M., Parsons, M.B., Seal, R.R., 2015. Characteristics and environmental aspects of slag: A review. Appl Geochem 57, 236–266. https://doi.org/10.1016/j.apgeochem.2014.04.009.
[40] Hudson-Edwards, K.A., Jamieson, H.E., Lottermoser, B.G., 2011. Mine wastes: past, present, future. Elements 7, 375–380. https://doi.org/10.2113/gselements.7.6.375.
[41] Ciesielczuk, J., Misz-Kennan, M., Hower, J.C., Fabiańska, M.J., 2014. Mineralogy and geochemistry of coal wastes from the Starzykowiec coal-waste dump (Upper Silesia, Poland). Int. J. Coal Geol. 127, 42–55. https://doi.org/10.1016/j.coal.2014.02.007.
[42] CCME, Canadian Council of Ministers of the Environment, 2007. Canadian Soil Quality Guidelines for the Protection of Environmental and Human Health. Excerpt from Publication No. 1299; ISBN 1-896997-34-1.
[43] Environment Agency, 2008. Assessment of Metal Mining-Contaminated River Sediments in England and Wales. Environment Agency, Bristol, UK.
[44] Wedepohl, K.H., 1995. The composition of the continental crust. Geochim Cosmochim Ac 59, 1217–1232. https://doi.org/10.1016/0016-7037(95)00038-2.
[45] Ander, E., Johnson, L., Cave, C.C., Palumbo-Roe, M.R., Nathanail, B., Lark, C.P., et al., 2013. Methodology for the determination of normal background concentrations of contaminants in English soil. Sci Total Environ 454–455, 604–618. https://doi.org/10.1016/j.scitotenv.2013.03.005.
[46] CCME, Canadian Council of Ministers of the Environment, 2001. Canadian Sediment Quality Guidelines for the Protection of Aquatic life: Summary Tables. Updates. In Canadian Council of Ministers of the Environment (CCME) (Ed.). *Canadian Sediment Quality Guidelines* (pp. 1-5). Environment Canada.
[47] Saxby, J.D., 2000. Minerals in coal. In: Glikson, M., Mastalerz, M. (Eds.), Organic Matter and Mineralisation: Thermal Alteration, Hydrocarbon Generation and Role in Metallogenesis. Springer, Dordrecht. https://doi.org/10.1007/978-94-015-9474-5_15.
[48] Ciesielczuk, J., Misz-Kennan, M., Hower, J.C., Fabiańska, M.J., 2014. Mineralogy and geochemistry of coal wastes from the Starzykowiec coal-waste dump (Upper Silesia, Poland). Int J Coal Geol 127, 42–55. https://doi.org/10.1016/j.coal.2014.02.00.
[49] Dai, S., Ren, D., Zhou, Y., Chou, C.-L., Wang, X., Zhao, L., et al., 2008. Mineralogy and geochemistry of a super high-organic-sulfur coal, Yanshan Coalfield, Yunnan, China: Evidence for a volcanic ash component and influence by submarine exhalation. Chem Geol 255, 182–194. https://doi.org/10.1016/j.chemgeo.2008.06.030.
[50] Hower, J.C., Wild, G.D., Pollock, J.D., Trinkle, E.J., Bland, A.E., Fiene, F.L., 1990. Petrography, geochemistry, and mineralogy of the Springfield (Western Kentucky No. 9) coal bed. J Coal Qual 9, 90–100.
[51] Hudson-Edwards, K.A., Macklin, M.G., Curtis, C.D., Vaughan, D.J., 1996. Processes of Formation and Distribution of Pb-, Zn-, Cd-, and Cu-Bearing Minerals in the Tyne Basin, Northeast England: Implications for Metal-Contaminated River Systems. Environ Sci Technol 30, 72–80. https://doi.org/10.1021/es9500724.
[52] Cidu, R., Dadea, C., Desogus, P., Fanfani, L., Manca, P.P., Orrù, G., 2012. Assessment of environmental hazards at abandoned mining sites: a case study in Sardinia, Italy. Appl Geochem 13th Int Symp WaterRock Interact (WRI 13) 27, 1795–1806. https://doi.org/10.1016/j.apgeochem.2012.02.014.
[53] Jennings, E., Onnis, P., Crane, R., Comber, S.D.W., Byrne, P., Riley, A.L., et al., 2025. Spatial and temporal (annual and decadal) trends of metal(loid) concentrations and loads in an acid mine drainage-affected river. Sci Total Environ 964, 178496. https://doi.org/10.1016/j.scitotenv.2025.178496.
[54] Piatak, N.M., Parsons, M.B., Seal, R.R., 2015. Characteristics and environmental aspects of slag: A review. Appl. Geochem. Environ. Geochem. Mod. Min. 57, 236–266. https://doi.org/10.1016/j.apgeochem.2014.04.009.
[55] Riley, A.L., MacDonald, J.M., Burke, I.T., Renforth, P., Jarvis, A.P., Hudson-Edwards, K.A., et al., 2020. Legacy iron and steel wastes in the UK: extent, resource potential, and management futures. J Geochem Explor 219, 106630. https://doi.org/10.1016/j.gexplo.2020.106630.
[56] Babich, A., Dieter, S., 2013. Biomass use in the steel industry: back to the future? Stahl und Eisen 133, 57–67.
[57] Artemyev, D.A., Ankushev, M.N., 2019. Trace elements of Cu-(Fe)-sulfide inclusions in Bronze Age copper slags from South Urals and Kazakhstan: ore sources and alloying additions. Minerals 9, 746. https://doi.org/10.20944/preprints201910.0011.v1.
[58] Alam, Q., Schollbach, K., Rijnders, M., van Hoek, C., van der Laan, S., Brouwers, H. J.H., 2019. The immobilisation of potentially toxic elements due to incineration and weathering of bottom ash fines. J Hazard Mater 379, 120798. https://doi.org/10.1016/j.jhazmat.2019.120798.
[59] Kjeldsen, P., Barlaz, M.A., Rooker, A.P., Baun, A., Ledin, A., Christensen, T.H., 2002. Present and long-term composition of MSW landfill leachate: a review. Crit Rev Env Sci Tec 32, 297–336. https://doi.org/10.1080/10643380290813462.
[60] Abramov, S., He, J., Wimmer, D., Lemloh, M.-L., Muehe, E.M., Gann, B., et al., 2018. Heavy metal mobility and valuable contents of processed municipal solid waste incineration residues from Southwestern Germany. Waste Manag 79, 735–743. https://doi.org/10.1016/j.wasman.2018.08.010.
[61] Williams, T.P., 2006. Waste Treatment and Disposal, second ed. Wiley Editorial Officer.
[62] Fendorf, S.E., 1995. Surface reactions of chromium in soils and waters. Geoderma 67, 55–71. https://doi.org/10.1016/0016-7061(94)00062-F.
[63] Watanabe, T., Jahan, P., Satoh, S., Kiron, V., 1999. Total phosphorus loading onto the water environment from common carp fed commercial diets. Fish Sci 65, 712–716. https://doi.org/10.2331/fishsci.65.712.
[64] Hu, H., Liu, H., Chen, J., Li, A., Yao, H., Low, F., Zhang, L., 2015. Speciation transformation of arsenic during municipal solid waste incineration. Proc. Combust. Inst. 35, 2883–2890. https://doi.org/10.1016/j.proci.2014.06.052.
[65] Bayuseno, A.P., Schmahl, W.W., 2010. Understanding the chemical and mineralogical properties of the inorganic portion of MSWI bottom ash. Waste Manag 30, 1509–1520. https://doi.org/10.1016/j.wasman.2010.03.010.
[66] Brand, J.H., Spencer, K.L., 2019. Potential contamination of the coastal zone by eroding historic landfills. Mar Pollut Bull 146, 282–291. https://doi.org/10.1016/j.marpolbul.2019.06.017.
[67] Paoletti, F., Sirini, P., Seifert, H., Vehlow, J., 2001. Fate of antimony in municipal solid waste incineration. Chemosphere 42, 533–543. https://doi.org/10.1016/S0045-6535(00)00225-3.
[68] Samal, S., Ray, A.K., Bandopadhyay, A., 2013. Proposal for resources, utilisation and processes of red mud in India — A review. Int J Miner Process 118, 43–55. https://doi.org/10.1016/j.minpro.2012.11.001.
[69] Reddy, T.P., Kishore, S.J., Theja, P.C., Punna Rao, P., 2020. Development and wear behavior investigation on aluminum-7075/B4C/fly ash metal matrix composites. Adv Compos Hybrid Mater 3, 255–265. https://doi.org/10.1007/s42114-020-00145-5.
[70] Liu, Y., Naidu, R., 2014. Hidden values in bauxite residue (red mud): recovery of metals. Waste Manag 34, 2662–2673. https://doi.org/10.1016/j.wasman.2014.09.003.

[71] Lockwood, C.L., Mortimer, R.J.G., Stewart, D.I., Mayes, W.M., Peacock, C.L., Polya, D.A., et al., 2014. Mobilisation of arsenic from bauxite residue (red mud) affected soils: Effect of pH and redox conditions. Appl Geochem 51, 268–277. https://doi.org/10.1016/j.apgeochem.2014.10.009.
[72] Mukherjee, T.K., Chakraborty, S.P., Bidaye, A.C., Gupta, C.K., 1990. Recovery of pure vanadium oxide from Bayer sludge. Miner Eng 3, 345–353.
[73] Ochsenkühn-Petropulu, M., Lyberopulu, Th, Ochsenkühn, K.M., Parissakis, G., 1996. Recovery of lanthanides and yttrium from red mud by selective leaching. Anal Chim Acta 319, 249–254. https://doi.org/10.1016/0003-2670(95)00486-6.
[74] Mosley, L.M., Liss, P.S., 2020. Particle aggregation, pH changes and metal behaviour during estuarine mixing: review and integration. Mar Freshw Res 71, 300. https://doi.org/10.1071/mf19195.
[75] UKCP09 (2009). *UK Climate Projections 2009. Met Office Hadley* Centre, Exeter, UK. Available at: ⟨https://ukclimateprojections.metoffice.gov.uk/⟩ (accessed 15 August 2024).
[76] Gandy, C.J., Burke, I.T., Byrne, P., Cooper, N., Crane, R.A., Hudson-Edwards, K.A., et al., 2025. Spatial variability of metal(loid) leaching from coastal colliery wastes under freshwater and saline water conditions. J Environ Manag 376, 124489. https://doi.org/10.1016/j.jenvman.2025.124489.
[77] Nordstrom, D.K., 2002. Worldwide occurrences of arsenic in ground water. Science 296, 2143–2145. https://doi.org/10.1126/science.1072375.
[78] Tuo, P., Zhang, Z., Du, P., Hu, L., Li, R., Ren, J., 2024. Changes in coal waste DOM chemodiversity and Fe/Al oxides during weathering drive the fraction conversion of heavy metals. Sci Total Environ 926, 172063. https://doi.org/10.1016/j.scitotenv.2024.172063.
[79] Lynch, S.F.L., Batty, L.C., Byrne, P., 2014. Environmental risk of metal mining contaminated river bank sediment at redox-transitional zones. Minerals 4, 52–73. https://doi.org/10.3390/min4010052.
[80] Mayes, W.M., Potter, H.A.B., Jarvis, A.P., 2013. Riverine flux of metals from historically mined orefields in England and Wales. Water Air Soil Pollut 224, 1425. https://doi.org/10.1007/s11270-012-1425-9.
[81] Macklin, M.G., Thomas, C.J., Mudbhatkal, A., Brewer, P.A., Hudson-Edwards, K.A., Lewin, J., et al., 2023. Impacts of metal mining on river systems: a global assessment. Science 381, 1345–1350. https://doi.org/10.1126/science.adg6704.
[82] Onnis, P., Byrne, P., Hudson-Edwards, P.A., Stott, T., Hunt, C.O., 2023. Fluvial morphology as a driver of lead and zinc geochemical dispersion at a catchment scale. Minerals 13, 790. https://doi.org/10.3390/min13060790.
[83] Onnis, P., Byrne, Patrick, Hudson-Edwards, Karen A., Frau, Ilaria, Stott, Tim, Williams, Tom, et al., 2023. Source apportionment of mine contamination across streamflows. Appl Geochem 151, 105623. https://doi.org/10.1016/j.apgeochem.2023.105623.
[84] Yao, F.X., Macíasc, F., Virgela, S., Blancoa, F., Jiangb, X., Camps Arbestaina, M., 2009. Chemical changes in heavy metals in the leachates from Technosols. Chemosphere 77, 29–35. https://doi.org/10.1016/j.chemosphere.2009.06.012.
[85] Angel, B.M., Apte, S.C., Batley, S.C., Raven, M.D., 2016. Lead solubility in seawater: an experimental study. Environ Chem 13, 489–495. https://doi.org/10.1071/EN15150.
[86] Flyhammer, P., Tamaddon, F., Bengtsson, L., 1998. Heavy metals in municipal solid waste deposition cell. Waste Manag Res 16, 403–410.
[87] Brand, J.H., Spencer, K.L., 2020. Will flooding or erosion of historic landfills result in a significant release of soluble contaminants to the coastal zone? Sci Total Environ 724, 138150. https://doi.org/10.1016/j.scitotenv.2020.138150.
[88] Lumpkin, G.R., 2001. Crystal chemistry and durability of the spinel structure type in natural systems. Prog Nucl Energ 38, 447–454.
[89] Botsou, F., Koutsopoulou, E., Andrioti, A., Dassenakis, M., Scoullos, M., Karageorgis, A.P., 2022. Chromium speciation, mobility, and Cr(VI) retention–release processes in ultramafic rocks and Fe–Ni lateritic deposits of Greece. Environ Geochem Health 44, 2815–2834. https://doi.org/10.1007/s10653-021-01078-8.
[90] Fandeur, D., Juillot, F., Morin, G., Olivi, L., Cognigni, A., Webb, S., et al., 2009. XANES evidence for oxidation of Cr(III) to Cr(VI) by Mn-oxides in a lateritic regolith developed on serpentinised ultramafic rocks in New Caledonia. Envir Sci Technol 43, 7384–7390. https://doi.org/10.1021/es900498r.
[91] Chen, L., Liu, J., Hu, W., Gao, J., Yang, J., 2021. Vanadium in soil-plant system: source, fate, toxicity, and bioremediation. J Hazard Mater 405, 124200. https://doi.org/10.1016/j.jhazmat.2020.124200.
[92] Burke, I.T., Mayes, W.M., Peacock, C.L., Brown, A.P., Jarvis, A.P., Gruiz, K., 2012. Speciation of arsenic, chromium, and vanadium in red mud samples from the Ajka Spill Site, Hungary. Environ Sci Technol 46, 3085–3092. https://doi.org/10.1021/es3003475.
[93] Gomes, H.I., Jones, A., Rogerson, M., Burke, I.T., Mayes, W.M., 2016. Vanadium removal and recovery from bauxite residue leachates by ion exchange. Environ Sci Pollut Res 23, 23034–23042. https://doi.org/10.1007/s11356-016-7514-3.
[94] Manning, B.A., Goldberg, S., 1996. Modelling competitive adsorption of arsenate with phosphate and molybdate on oxide minerals. Soil Sci Soc Am J 60, 121–131. https://doi.org/10.2136/sssaj1996.03615995006000010020x.